

The Conformation of Alkyl Benzyl Alcohols Studied by ab initio MO Calculations – A Comparison with IR and NMR Spectroscopic Data

Osamu Takahashi,^{*,[a]} Ko Saito,^[a] Yuji Kohno,^[b] Hiroko Suezawa,^{*,[c]} Shinji Ishihara,^[c] and Motohiro Nishio^{*,[d]}

Keywords: CH/ π interaction / OH– π interaction / Nuclear Overhauser effect / Vicinal coupling constant / Infrared spectra

Ab initio MO calculations were carried out for the conformations of a series of alkyl-substituted benzyl alcohols $C_6H_5CH_2CHOH-R$ ($R = CH_3, C_2H_5, iPr, tBu$) at the MP2/6-311G(d,p)//MP2/6-31G(d) level. It was found that the conformation where the OH group is *gauche* to the phenyl group is the most stable. The geometry where both the OH and R groups are close to phenyl is the second most stable. This finding has been interpreted on the grounds of the attractive

OH/ π and CH/ π hydrogen bonds and a repulsive van der Waals interaction between vicinal CH groups. NMR nuclear Overhauser effects, spin-coupling data, and IR spectroscopic data are consistent with the conclusion given by the MO calculations.

(© Wiley-VCH Verlag GmbH & Co. KGaA, 69451 Weinheim, Germany, 2004)

Introduction

Previously, we studied the conformation of a series of benzylic compounds $C_6H_5CH_2XR$ ($X = O, CH_2, CO, S, SO$, and SO_2) using ab initio MO calculations at the MP2/6-311G(d,p)//MP2/6-31G(d) level.^[1] The most stable conformation was shown to have R and C_6H_5 in a synclinal relationship, although there were exceptions for several analogues bearing a *tert*-butyl group. In order to account for those results, we suggested that there is an important contribution from the CH/ π hydrogen bond. In this work, we have used the ab initio MO method to analyze the conformation of the structurally related alcohols $C_6H_5CH_2CHOH-R$: 1-phenyl-2-propanol **1** ($R = CH_3$), 1-phenyl-2-butanol **2** ($R = C_2H_5$), 3-methyl-1-phenyl-2-butanol **3** ($R = iPr$), and 3,3-dimethyl-1-phenyl-2-butanol **4** ($R = tBu$). These benzylic alcohols **1–4** differ from the molecules previously reported in that the OH/ π hydrogen bonding may occur in certain geometries. It is interesting to compare the effect of the two types of π -hydrogen bonds (CH/ π ^[2,3] vs. OH/ π ^[4,5]) in these aralkyl compounds.

Results and Discussion

Figure 1 shows that, in **1–4**, three geometries are possible by rotation about the central C–C bond (ϕ). Additionally, the OH group is free to rotate about the HO–C bond (ψ) to give three further rotational isomers. For the ethyl and isopropyl analogues (**2** and **3**, respectively), we must consider the rotation about the C–C–CH₃ bond in R (ω). Accordingly, the number of possible conformations is 9 for $R = CH_3$ **1** and *tBu* **4**, and 27 for $R = C_2H_5$ **2** and *iPr* **3**.

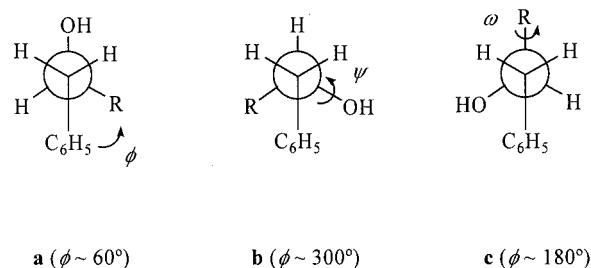


Figure 1. Rotamers of **1–4**; three possible geometries are obtained by rotation about the central C–C bond (ϕ); the OH group may rotate about the HO–C bond (ψ); for **2** ($R = C_2H_5$) and **3** ($R = iPr$), rotation about the C–C–CH₃ bond in R (ω) is possible

Conformational Energy

The energy profiles obtained for **1** at the MP2/6-31G(d) level are given in Figure 2. It is clear from Figure 2 (a) that **1** exists in three stable conformations (**a**, **b**, and **c**) by rotation of the $C_6H_5-C-C-R$ bond (ϕ). Figure 2 (b) shows

^[a] Department of Chemistry, Graduate School of Science, Hiroshima University, Kagamiyama, 1-3-1, Higashi-Hiroshima 739–8526, Japan
E-mail: shu@hiroshima-u.ac.jp

^[b] Shock Wave Research Center, Institute of Fluid Science, Tohoku University, 2-1-1 Katahira, Aoba-ku, Sendai 980–8577, Japan

^[c] Instrumental Analysis Center, Yokohama National University, Hodogaya-ku, Yokohama 240–8501, Japan
E-mail: suezawa@ynu.ac.jp

^[d] The CHPI Institute, 3-10-7 Narusedai, Machida-shi, Tokyo 194–0043, Japan
E-mail: dionisio@tim.hi-ho.ne.jp

that each rotamer has three stable geometries derived from rotation about C–C–O–H (ψ).

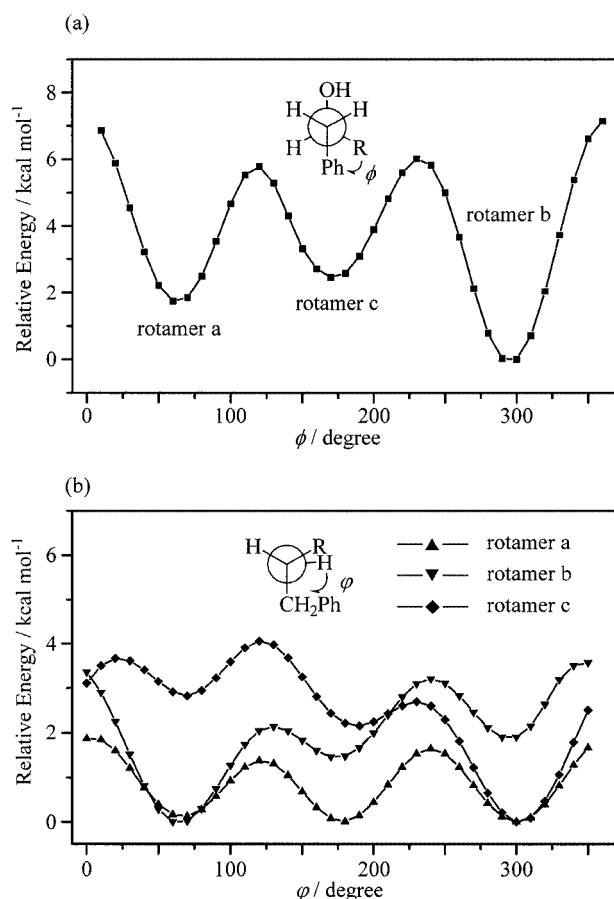


Figure 2. Energy profiles obtained for **1** ($R = \text{CH}_3$) at the MP2/6-31G(d) level: (a) three stable conformations **a**, **b**, and **c** obtained by rotation of the $\text{C}_6\text{H}_5\text{--C--C--R}$ bond (ϕ) are shown; note that the result differs from that reported in Table 1 since, in this preliminary survey, the C–C–O–H angle (ψ) was fixed at a constant value; (b) three stable geometries for conformations **a**, **b**, and **c** obtained by rotation about ψ are shown

Table 1 lists the relative Gibbs energy of the stable conformations of these alcohols. Table 2 shows the effect of the basis set used in the calculations on the relative steric energy of the methyl analogue **1**. For this, the geometry of the rotamers optimized at the MP2/6-31G(d) level was used. The variation in steric energies is insignificant and the order of rotamers does not vary from method to method. Notice that in rotamer **a**, where OH/ π bonding cannot occur, the energy levels of the three wells are comparable, while in rotamers **b** and **c**, we see that one of the three geometries is appreciably more stable than the other two. This is because the stabilizing OH/ π interaction is operating in these geometries.

Perusal of Table 1 demonstrates that one of the rotamers corresponding to geometry **c** is the most stable in every case. In this rotamer, R is *anti* to the phenyl group (ϕ 178° for **1–3** and 180° for **4**). The stability of rotamer **c** can be ascribed to the OH/ π interaction. Stabilization by CH/ π interactions may occur in rotamers **a** and **b**.

Table 1. Relative conformational Gibbs energies (in order of increasing magnitude with respect to the most stable one: in *italics*) of the conformations of alkyl benzyl alcohols $\text{C}_6\text{H}_5\text{CH}_2\text{CHOH--R}$ **1–4** calculated by the ab initio method [MP2/6-311G(d,p)//MP2/6-31G(d)]; optimized torsion angles R/Ph (ϕ°) are given in parentheses; for **2** and **3**, only the most stable geometries at a given angle around the C–C–CH₃ bond in R (ω) are given

1 $R = \text{CH}_3$

rotamer a	1.10 (64); 1.11 (63); 1.18 (64)
rotamer b	0.48 (295); 1.18 (307); 1.50 (309)
rotamer c	0.00 (178); 1.41 (173); 1.59 (172)

2 $R = \text{C}_2\text{H}_5$

rotamer a	1.08 (64); 1.16 (65); 1.66 (61); 1.66 (61); 1.78 (62); 2.05 (60); 2.65 (65); 2.67 (63); 2.80 (61)
rotamer b	0.51 (295); 1.04 (296); 1.45 (309); 1.53 (306); 1.66 (311); 2.32 (312); 3.24 (296); 3.37 (304); 3.69 (305)
rotamer c	0.00 (178); 0.68 (177); 0.76 (179); 1.62 (170); 1.66 (172); 1.98 (168); 2.04 (173); 2.23 (173); 2.67 (166)

3 $R = i\text{Pr}$

rotamer a	0.71 (65); 1.53 (49); 1.71 (48); 2.36 (65); 2.71 (57); 2.95 (56); 3.18 (56); 3.64 (69); 3.84 (56)
rotamer b	0.93 (299); 1.11 (300); 1.13 (301); 2.81 (296); 3.14 (296); 3.04 (285); 3.15 (281); 3.34 (297); 3.36 (282)
rotamer c	0.00 (178); 0.06 (175); 0.39 (180); 1.40 (165); 1.70 (170); 1.81 (171); 1.81 (178); 1.83 (164); 2.35 (165)

4 $R = t\text{Bu}$

rotamer a	3.26 (69); 3.22 (58); 3.42 (57)
rotamer b	3.29 (294); 3.38 (295); 3.42 (295)
rotamer c	0.00 (180); 1.53 (165); 1.88 (168)

Conformational Equilibrium

In this section, we consider the rotameric abundance (grouped into categories **a**, **b**, and **c**) rather than the stability of each rotamer since the large number of possible rotamers makes a complete survey difficult. Table 3 summarizes the abundance of the three rotamers which was estimated according to the Gibbs energies listed in Table 1. In every case, rotamer **c** is the most abundant, followed by rotamer **b** and then **a**. The proportion of rotamer **c** gradually increases passing from **1** to **2** and then **3**. In **4**, this is almost the only rotamer present at equilibrium.

The above result can be explained in terms of the compromise between various effects, which are caused by weak intramolecular forces. These include the OH/ π and CH/ π hydrogen bonds and unfavorable steric (repulsive van der Waals) interactions, which can occur between vicinal CH groups. Thus, the OH/ π interaction can operate in both rotamers **b** and **c**. The OH/ π and CH/ π hydrogen bonds can operate simultaneously in rotamer **b**. However, in rotamer

Table 2. Relative conformational Gibbs energies (with respect to the most stable one: in *italics*) of the stable conformations of 1-phenyl-2-propanol $C_6H_5CH_2CHOHCH_3$ **1** calculated using various levels of theory; optimized torsion angles R/Ph (φ°) are given in parentheses;^[a] each three values correspond to the differing rotation angle around the HO–C bond (ψ)

MP2/6-31G(d)	
rotamer a	1.99 (64); 2.10 (63); 1.98 (64)
rotamer b	0.30 (295); 1.77 (307); 2.20 (309)
rotamer c	0.00 (178); 2.16 (173); 2.83 (172)
MP2/6-31G(d,p)	
rotamer a	1.83 (64); 1.88 (63); 1.74 (64)
rotamer b	0.25 (295); 1.62 (307); 1.96 (309)
rotamer c	0.00 (178); 2.03 (173); 2.67 (172)
MP2/6-311G(d,p)	
rotamer a	1.43 (64); 2.21 (63); 1.47 (64)
rotamer b	0.04 (295); 1.31 (307); 1.64 (309)
rotamer c	0.00 (178); 2.29 (173); 1.96 (172)
MP2/6-311++G(d,p)	
rotamer a	1.29 (64); 1.61 (63); 1.24 (64)
rotamer b	0.71 (295); 1.48 (307); 2.05 (309)
rotamer c	0.00 (178); 2.91 (173); 2.08 (172)

^[a] Geometry optimized at the MP2/6-31G(d) level is given.

Table 3. Relative abundance (%) of the stable conformations of alkyl benzyl alcohols $C_6H_5CH_2CHOH-R$ **1–4** calculated by the ab initio method [MP2/6-311G(d,p)//MP2/6-31G(d)]. Data are grouped into three geometries **a**, **b**, and **c** with respect to the rotation of the central C–C bond (φ).

R	Rotamer a	Rotamer b	Rotamer c
CH ₃	19.7	29.0	51.3
C ₂ H ₅	17.7	26.1	56.2
<i>i</i> Pr	12.7	14.3	73.0
<i>t</i> Bu	1.0	0.9	98.1

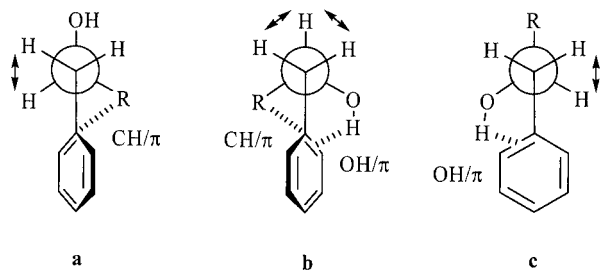


Figure 3. Rotamers of benzylic alcohols $C_6H_5CH_2CHOH-R$ **1–4** and possible interactions involved; arrows show unfavorable vicinal H/H interactions; the putative OH/π and CH/π interactions are indicated by dotted lines; note that CH interacts with H_{ipso} while OH points towards the approximate midpoint of H_{ipso} and H_{ortho}

b, there are also two unfavorable H/H interactions. According to Allinger, the steric congestion between vicinal CH groups is very severe.^[6] CH/π interactions can operate in

rotamer **a**, while stabilization from the OH/π interaction is not anticipated. Figure 3 shows interactions (attractive as well as repulsive) present in rotamers **a**, **b**, and **c**.

Interatomic Distances

Table 4 compiles the distances at the CH/π- ($d1$, $d2$) and OH/π-interacting geometries ($d3$ – $d5$). Notice that these values are smaller than the sum of the van der Waals radii of the relevant atoms. In every case, the distance between the OH hydrogen and the midpoint of C_{ipso} and C_{ortho} (OH/ $C_{midpoint}$: $d4$) is shorter than the OH/ C_{ipso} ($d3$) and OH/ C_{ortho} ($d5$) distances. This suggests that the OH group prefers to interact with the *ortho* carbon or at a point close to the midpoint between the two carbons. Oki and Iwamura have already noted the possibility of bifurcated OH/π bonding, by analyzing electronic substituent effects on the infrared O–H stretching band of 2-phenylethyl alcohol derivatives.^[7]

Table 4. Interatomic CH/C and OH/C distances (Å) of the stable conformations of benzylic alcohols $C_6H_5CHCH_3CHOH-R$ **1–4** calculated by the ab initio method: MP2/6-311G(d,p)//MP2/6-31G(d); $d1$: distance between CH and C_{ipso} ; $d2$: CH/ C_{ortho} ; $d3$: distance between OH and C_{ipso} ; $d4$: OH/ $C_{midpoint}$; $d5$: OH/ C_{ortho}

φ°	CH/π distance		OH/π distance		
	$d1$	$d2$	$d3$	$d4$	$d5$
1 R = CH₃					
64 (a)	2.774	2.931			
64	2.778	2.931			
63	2.774	2.937			
295 (b)	2.788	2.828	2.595	2.455	2.512
307	2.683	3.034			
309	2.685	3.133			
178 (c)			2.498	2.406	2.514
2 R = C₂H₅					
64 (a)	2.706	2.862			
65	2.708	2.857			
61	2.748	3.063			
296 (b)	2.766	2.818	2.588	2.444	2.497
295	2.774	2.817	2.573	2.434	2.493
296	2.665	2.664	2.679	2.500	2.512
177 (c)			2.469	2.384	2.502
178			2.501	2.408	2.515
179			2.490	2.395	2.502
3 R = <i>i</i>Pr					
65 (a)	2.771	2.819			
49	2.635	2.946			
48	2.503	2.854			
285 (b)	2.559	2.646	2.553	2.409	2.464
281	2.637	2.660	2.664	2.474	2.476
282	2.612	2.652	2.677	2.499	2.512
175 (c)			2.434	2.358	2.486
180			2.466	2.401	2.492
178			2.500	2.401	2.503
4 R = <i>t</i>Bu					
69 (a)	2.639	2.605			
57	2.540	2.824			
58	2.542	2.750			
294 (b)	2.532	2.673	2.650	2.458	2.461
295	2.522	2.693			
295	2.537	2.670			
180 (c)			2.433	2.350	2.473

In contrast, the distance $\text{CH}/C_{\text{ipso}}$ d_1 is usually shorter than the $\text{CH}/C_{\text{ortho}}$ distance d_2 . This shows that CH/π bonding occurs at the *ipso* carbon of the phenyl group. A plausible explanation is that the nature of the OH/π hydrogen bond is somewhat different from that of the CH/π hydrogen bond. Actually, it has been suggested that the contribution from the electrostatic force is larger in the OH/π than in the CH/π hydrogen bond.^[5a]

Comparison with Spectroscopic Data

IR Spectroscopic Data

Kodama et al. determined IR spectra of a series of 1-phenylethyl alcohols $\text{C}_6\text{H}_5\text{CHCH}_2\text{CHOH}-\text{R}$ ^[8] and reported that the OH/π -bonding peak appears at $3596\text{--}3614\text{ cm}^{-1}$, whereas that of the free species appears at $3629\text{--}3648\text{ cm}^{-1}$. In Figure 4 the relevant region of the IR spectra of **1–4** is shown. The peaks ascribed to the OH/π -bonded species ($3600\text{--}3606\text{ cm}^{-1}$) are red-shifted by ca. 25 cm^{-1} relative to the nonbonded ones ($3624\text{--}3630\text{ cm}^{-1}$). The relative intensity of the lower frequency band increases going from **1** to **2**, **3**, and then **4**. The result is consistent with the relative abundance of rotamer **c** estimated by the MO method.

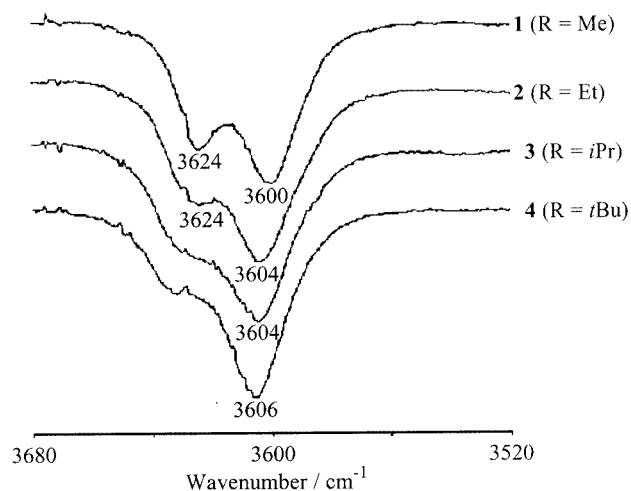


Figure 4. Infrared spectra of **1–4** obtained from CCl_4 solutions

Nuclear Overhauser Effects

In order to obtain support for the suggestion made above, we determined the nuclear Overhauser effects (NOE) present in **1–4**. It is known that NOE enhancement reflects the distance between the interacting protons. In Figure 5, the hydrogen α to the OH group is labeled H_x . For the benzylic hydrogens (β to OH), the signal appearing at lower field is labeled H_a , while the more shielded one is labeled H_b .

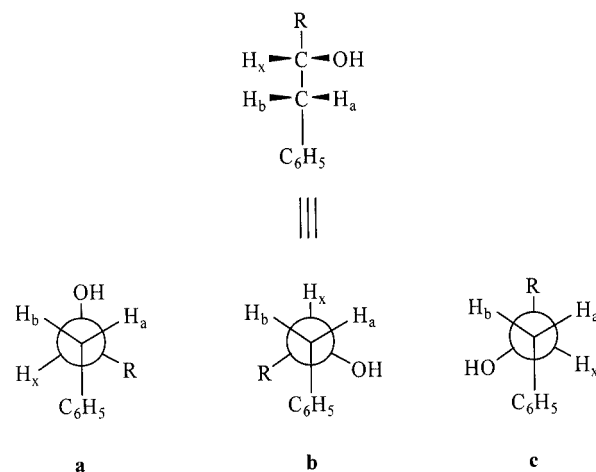


Figure 5. Relative geometrical disposition of H_x , H_a , and H_b in rotamers **a**, **b**, and **c**

According to Table 3, rotamer **c** is the most abundant of the three rotamers. As shown in Figure 5, H_a is close (*cis*) to H_x in rotamer **c**, while H_b is remote (*trans*) from H_x . Therefore, the NOE enhancement of H_a is expected to be larger than H_b when H_x is irradiated if rotamer **c** is highly populated. Table 5 gives the NOE data.

Table 5. NMR spectroscopic data for 1-phenyl-2-propanol **1**, 1-phenyl-2-butanol **2**, 3-methyl-1-phenyl-2-butanol **3**, and 3,3-dimethyl-1-phenyl-2-butanol **4** determined in CDCl_3 solutions

	1	2	3	4
Chemical shift ^[a]				
H_x	4.03	3.75	3.59	3.44
H_a	2.80	2.84	2.86	2.92
H_b	2.69	2.65	2.60	2.45
NOE ^[b]				
H_a	2.3	2.3	2.5	2.7
H_b	1.4	1.3	1.1	0.5
Ratio (H_a/H_b)	1.5	1.6	2.3	5.4

^[a] ppm downfield from internal TMS. ^[b] Percentage of the NOE enhancement by irradiating H_x .

The ratio $\text{NOE}_{\text{Ha}}/\text{NOE}_{\text{Hb}}$ increases from 1.5 for **1**, to 1.6 for **2** and 2.3 for **3**, and finally to 5.4 for **4**. There is satisfactory agreement between the NOE data and the abundances of rotamer **c** in **1–4** reported in Table 3.

Consideration of the Vicinal Spin-Coupling Constant

Table 6 lists the vicinal spin-coupling constants of the alcohols.

Table 6. Coupling constants (in Hz) of 1-phenyl-2-propanol **1**, 1-phenyl-2-butanol **2**, 3-methyl-1-phenyl-2-butanol **3**, and 3,3-dimethyl-1-phenyl-2-butanol **4** determined in CDCl_3 solutions

	1	2	3	4
$^3J_{\text{HaHx}}$	4.95	4.62	3.63	1.98
$^3J_{\text{HbHx}}$	7.85	8.20	9.24	10.88

The spin-coupling constant between vicinal hydrogens H_a and H_x ($^3J_{HaHx}$) is smaller, in every case, than $^3J_{HbHx}$. The $^3J_{HaHx}$ value gradually decreases on going from **1** (4.95 Hz) to **2**, **3**, and then drops abruptly to 1.98 Hz in **4**. An opposite trend was recorded for $^3J_{HbHx}$. We plotted $^3J_{HbHx}$ and $^3J_{HaHx}$ against the computed rotamer populations. This gave good linear correlation ($R > 0.99$; not shown). The result is compatible with the expectation that rotamer **c** prevails in solutions of **1–3** and is almost the only conformation in **4**.

Calculation of the Vicinal Coupling Constants $^3J_{trans}$ and $^3J_{cis}$

Using the rotamer populations reported in Table 3, vicinal coupling constants $^3J_{trans}$ and $^3J_{cis}$ were computed. The following relationships were obtained from the equilibrium data of **1**.

$$^3J_{HaHx}: 19.7 \times J_{trans} + (29.0 + 51.3) \times J_{cis} = 4.95 \times 100$$

$$^3J_{HbHx}: (19.7 + 29.0) \times J_{cis} + 51.3 \times J_{trans} = 7.85 \times 100$$

This gives 12.32 and 3.14 Hz for J_{trans} and J_{cis} respectively. The same procedure was applied to **2**, **3**, and **4** to give the results reported in Table 7. These values (11.9–12.32 Hz for J_{trans} and 1.89–3.14 Hz for J_{cis}) are compatible with those expected from the Karplus relationship.^[9]

Table 7. Coupling constants $^3J_{H,H}$ (in Hz) of *trans* and *cis* vicinal CHs calculated from the rotamer distributions listed in Table 3

	1	2	3	4	Average
J_{trans}	12.32	12.27	11.75	11.09	12.86
J_{cis}	3.14	2.97	2.45	1.89	2.61

Comparison of the Rotamer Abundance Obtained by ab initio Calculations with that Estimated from NMR Spin-Coupling Data

Next we calculated the rotameric abundance using the coupling parameters obtained above (average values). As shown in Figure 5, H_a is *trans* to H_x in rotamer **a**, while H_a is *cis* to H_x in rotamers **b** and **c**. On the other hand, H_b is *trans* to H_x in rotamer **a** and **b**, but is *cis* in rotamer **c**. Thus, for **1**, the following relationships [Equations (1)–(3)] stand.

$$a \times 12.9 + (b + c) \times 2.6 = 7.85 \times 100 \quad (1)$$

$$(a + b) \times 2.6 + c \times 12.9 = 4.95 \times 100 \quad (2)$$

$$a + b + c = 100 \quad (3)$$

Here, a , b , and c are the percentages of rotamers **a**, **b**, and **c**, respectively. This gives $a = 25.3$, $b = 18.1$, and $c =$

56.6. The results are summarized in Table 8. These values are in good agreement with those given in Table 3.

Table 8. Estimated rotamer distributions of **1–4** on the basis of the calculated coupling parameters

R	Rotamer a	Rotamer b	Rotamer c
CH ₃ 1 ^[a]	25.3	18.1	56.6
C ₂ H ₅ 2 ^[a]	21.7	17.9	60.4
<i>i</i> Pr 3 ^[a]	11.1	17.3	71.4
<i>t</i> Bu 4 ^[b]	—	10.6	89.4

^[a] Calculated by assuming 12 Hz for J_{trans} and 3 Hz for J_{cis} . ^[b] 11 Hz for J_{trans} , 2 Hz for J_{cis} .

Conclusions

In summary, ab initio calculations on benzylic alcohols gave results consistent with IR and NMR spectroscopic data. The importance of the OH/ π and CH/ π hydrogen bonds in controlling the conformation of aralkyl alcohols has been proposed. The present finding shows that ab initio calculations can be used with confidence to predict the conformation of simple organic molecules. Recognition of weak hydrogen bonds such as the OH/ π and CH/ π interactions is essential in elucidating stereochemical issues in aralkyl compounds.

Experimental Section

Methods

Computations: The GAUSSIAN 98 program^[10] was used. Electron correlation energies were calculated by applying the second order Møller-Plesset (MP2) perturbation theory. Geometry of the molecules was optimized at the MP2/6-31G(d) level of approximation. Using these geometries, single-point calculations were carried out at the MP2/6-311G (d,p) level to estimate the conformational energies. 6-31G(d), 6-31G(d,p), 6-311G(d,p) and 6-311G++(d,p) basis sets were also used for the calculation of **1** in order to examine the basis set dependence at the optimized geometry. Vibrational frequencies were calculated using the analytical second derivatives at the same level of the geometry optimization for each conformer. Using these results, the thermal energy corrections were added to the total energy at 298.15 K and 1 atmosphere of pressure, using the principal isotope for each element type.

Spectral Measurements: Infrared spectra were obtained from CCl₄ solutions using a Perkin–Elmer Spectrum 2000 infrared spectrophotometer. The concentration of the sample solution was always below 3×10^{-3} mol·dm^{−3}.

¹H NMR and NOE spectra were determined in CDCl₃ at 25 °C using a JEOL EX-270 spectrometer. In order to preclude effects from associated species, the concentration of the solution was maintained at less than 0.1 mol·dm^{−3}. The absence of associated species was confirmed by a dilution experiment; the downfield shift for δ (OH) was < 0.005 ppm from 0.2 to 2.5×10^{-3} mol·dm^{−3}. This is in the range of normal unassociated alcohols. The NOE values are the average of three measurements under different con-

ditions. The accumulation time, irradiation power (db), and irradiation time (s) were 64, 390, and 8 for the first run; 64, 385, and 7 for the second run; and 32, 380, and 7 for the third run, respectively. The coupling constants are accurate to ± 0.03 Hz.

Acknowledgments

The authors thank the Institute for Non-linear Science and Applied Mathematics at Hiroshima University for the use of an NEC HSP, the Information Media Center at Hiroshima University for the use of an H9000 VR360, and the Research Center for Computational Science, Okazaki National Research Institutes for the use of a Fujitsu VPP5000.

- [1] O. Takahashi, Y. Kohno, K. Saito, M. Nishio, *Chem. Eur. J.* **2003**, *9*, 756–762.
- [2] M. Nishio, M. Hirota, Y. Umezawa, *The CH/π Interaction. Evidence, Nature, and Consequences*, Wiley-VCH, New York, **1998**; M. Nishio, *CrystEngComm* **2004**, *6*, in press. A comprehensive literature list for the CH/π interaction is available at <http://www.tim.hi-ho.ne.jp/dionisio>
- [3] Recent MO studies include: [3a] J. J. Novoa, F. Mota, *Chem. Phys. Lett.* **2000**, *318*, 345–354. [3b] S. Tsuzuki, K. Honda, T. Uchimaru, M. Mikami, K. Tanabe, *J. Am. Chem. Soc.* **2000**, *122*, 3746–3753. [3c] A. Bagno, G. Saielli, G. Scorrano, *Angew. Chem. Int. Ed.* **2001**, *40*, 2532–2534. [3d] K. Sundararajan, K. Sankaran, K. S. Viswanathan, A. D. Kulkarni, S. R. Garde, *J. Phys. Chem. A* **2002**, *106*, 1504–1510. [3e] S. Scheiner, S. J. Grabowski, *J. Mol. Struct.* **2002**, *615*, 209–218. [3f] F. Ugozzoli, A. Arduini, C. Massera, A. Pochini, A. Secchi, *New J. Chem.* **2002**, *26*, 1718–1723. [3g] O. Takahashi, Y. Kohno, K. Saito, *Chem. Phys. Lett.* **2003**, *378*, 509–515.
- [4] [4a] M.-L. Josien, G. Sourisseau, *Hydrogen Bonding* (Ed. D. Hadzi), Pergamon Press, London, **1959**, 129–137. [4b] M. Oki, *Kagaku no Ryoiki* **1959**, *13*, 839–847. [4c] Z. Yoshida, E. Osawa, *Kagaku no Ryoiki* **1960**, *14*, 163–173, 248–254.
- [5] Recent ab initio study: [5a] S. Tsuzuki, K. Honda, T. Uchimaru, M. Mikami, K. Tanabe, *J. Am. Chem. Soc.* **2000**, *122*, 11450–11458. [5b] P. Tarakeshwar, K. S. Kim, *J. Mol. Struct.* **2002**, *615*, 227–238.
- [6] D. H. Wertz, N. L. Allinger, *Tetrahedron* **1974**, *30*, 1579–1586. In concluding remarks of this paper, the authors noted that “What causes the *gauche* H/H interaction to be so important is not so much its size, but rather the fact that unlike most of the other steric interactions one sees when one looks at a model of a compound the *gauche* H/H interaction can generally not be significantly reduced by any kind of molecular distortion.”
- [7] M. Oki, H. Iwamura, *Bull. Chem. Soc. Jpn.* **1959**, *32*, 1135–1143.
- [8] Y. Kodama, K. Nishihata, S. Zushi, M. Nishio, J. Uzawa, K. Sakamoto, H. Iwamura, *Bull. Chem. Soc. Jpn.* **1979**, *52*, 2661–2669.
- [9] M. Karplus, *J. Chem. Phys.* **1959**, *30*, 11–15. M. Karplus, *J. Am. Chem. Soc.* **1963**, *85*, 2870–2871.
- [10] M. J. Frisch, G. W. Trucks, H. B. Schlegel, G. E. Scuseria, M. A. Robb, J. R. Cheeseman, V. G. Zakrzewski, J. A. Montgomery, Jr., R. E. Stratmann, J. C. Burant, S. Dapprich, J. M. Millam, A. D. Daniels, K. N. Kudin, M. C. Strain, O. Farkas, J. Tomasi, V. Barone, M. Cossi, R. Cammi, B. Mennucci, C. Pomelli, C. Adamo, S. Clifford, J. Ochterski, G. A. Petersson, P. Y. Ayala, Q. Cui, K. Morokuma, D. K. Malick, A. D. Rabuck, K. Raghavachari, J. B. Foresman, J. Cioslowski, J. V. Ortiz, A. G. Baboul, B. B. Stefanov, G. Liu, A. Liashenko, P. Piskorz, I. Komaromi, R. Gomperts, R. L. Martin, D. J. Fox, T. Keith, M. A. Al-Laham, C. Y. Peng, A. Nanayakkara, C. Gonzalez, M. Challacombe, P. M. W. Gill, B. Johnson, W. Chen, M. W. Wong, J. L. Andres, C. Gonzalez, M. Head-Gordon, E. S. Replogle, J. A. Pople, *Gaussian 98, Revision A.4*, Gaussian, Inc., Pittsburgh, PA, **1998**.

Received December 22, 2003